Journal Name

ARTICLE

Synthesis of heterobimetallic gold(I) ferrocenyl-substituted 1,2,3-triazol-5-ylidene complexes as potential anticancer agents

Received 00th January 20xx,
Accepted 00th January 20xx

DOI: 10.1039/x0xx00000x

www.rsc.org/

Danielle Aucamp,[a],[b] Sreedhar V. Kumar,[a] David C. Liles,[b] Manuel A. Fernandes,[a] Leonie Harmse[c] and Daniela I. Bezuidenhout*[a]

1,2,3-Triazol-5-ylidene (trz) complexes of gold(I) containing a ferrocenyl substituent on the C4-position of the trz ring were synthesized to yield the neutral heterobimetallic gold(I) trz chlorido (**2**), gold(I) trz phenyl (**3**), and the cationic gold(I) trz triphenylphospine (**5**) complexes. In order to compare the effect of silver(I) as central metal vs. gold(I), $[Ag(trz)_2]^+$ (**4**) was also prepared, while variation of the C4-1,2,3-triazol-5-ylidene substituent from a ferrocenyl to a phenyl group was done to prepare the monometallic analogue of **5**, namely the cationic Au(I) trz triphenylphosphine complex **6**. The complexes were characterised with spectroscopic and electrochemical methods, and the single crystal X-ray structures of **2**–**6** were determined. NMR stability studies of **5** as a representative example of the series of complexes were performed to confirm the stability of the complexes in the solvent dimethylsulfoxide and in aqueous solution. The anti-cancer potential of **5** was evaluated against the lung cancer cell lines A549 and H1975, and the human embryonic kidney cell line (HEK-293) was used as a non-cancer model. IC_{50} values of 0.89, 0.23 and 5.43 µM, respectively, were obtained for A549, H1975 and HEK-293, respectively, indicating the activity and selectivity of **5** for cancer cells. Fluorescence microscopy experiments as a preliminary mode-of-action study evidenced an apoptotic cell death mechanism rather than necrotic cell death.

Introduction

The development of heterobimetallic complexes have received considerable attention in the recent past owing to their ability to exert improved biological activity compared to their monometallic counterparts.[1-4] Incorporation of two metal moieties in a heterobimetallic complex has proven to be an effective strategy to counteract resistance mechanisms whereby the activity exerted by each metal center results in activity against more than one cellular target in cancer cells.[5] Furthermore, the synergistic effect of two metal centers in a heterobimetallic complex would not only lead to enhanced activity but improve their stability and selectivity against cancer cells.[3]

Although the anticancer properties of ferrocene,[6-10] gold(I) N-heterocyclic carbene (NHC) complexes[11-14] and heterobimetallic gold(I) complexes[3,5] are well known, heterobimetallic gold(I) carbene complexes bearing a metallocenyl derivative are less explored for this application.

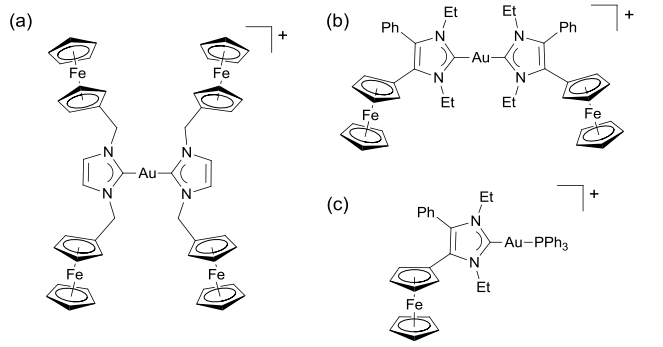

Fig. 1 Gold(I) ferrocenyl-substituted carbene complexes with reported anticancer activity.

Recent examples of this class of compounds are illustrated in Fig. 1 and are known to induce apoptosis in cancer cells by the production of reactive oxygen species (ROS), and by impedance of the thioredoxin reductase (TxR) enzyme.[15, 16]

The anticancer activity of a tetraferrocenylated biscarbene gold(I) complex against a series of cancer cell lines was reported by Arambula and co-workers (Fig. 1 (a)).[15] They have demonstrated that the heterometallic tetraferrocenylated gold complex displays improved anticancer activity compared to the diferrocenylated, or the monometallic gold(I) complex analogue. The improved activity was ascribed to the ability of the heterometallic complex to target antioxidant pathways in cancer cells.[15] Following this work, Casini and co-workers

[a] *Molecular Sciences Institute, School of Chemistry, University of the Witwatersrand, Johannesburg 2050, South Africa*
[b] *Chemistry Department, University of Pretoria, Private Bag X20, Hatfield 0028, Pretoria, South Africa .*
[c] *Division of Pharmacology, Department of Pharmacy and Pharmacology, Faculty of Health Sciences, University of the Witwatersrand, 7 York Road, Parktown, 2193, South Africa.*

† Electronic Supplementary Information (ESI) available: NMR spectra, cyclic voltammograms and crystal data. CCDC 1858615-1858619. See DOI: 10.1039/x0xx00000x

reported on the anticancer properties of cationic gold(I) ferrocenyl biscarbene and the triphenylphosphine complexes (Fig. 1 (b) and (c)).[16] In this case, the activity of the complexes was attributed not only to their ability to inhibit TxR enzyme but also to the increased levels of ROS in the cellular environment.[16]

A decade after their discovery,[17] 1,2,3-triazolylidenes have been widely exploited as excellent ligands towards the development of catalytically important organometallic complexes, due to the ability of these mesoionic carbenes to stabilise metals in either high or low oxidation states and their robust, donating nature upon metal complexation.[18-22] The versatility in the functionalisation of these ligands, mediated by modular click chemistry protocols, paved the way for the use of 1,2,3-triazolylidene ligands towards the syntheses of complexes with photophysical application,[23-26] or, more rarely, as organometallic anticancer agents. In this area, the limited reports include a cobaltocenium-appended 1,2,3-triazol-5-ylidene (trz) gold(I) complex, evaluated for its cytotoxic properties by Sarkar et al.,[27] as well as ruthenium(II) and osmium(II) trz complexes reported by Dyson et al.[28] As part of our recent interest towards the development of therapeutically important trz metal complexes, we herein report the syntheses and preliminary anticancer properties of a series of heterobimetallic 4-ferrocenyl-1,2,3-triazol-5-ylidene complexes of gold(I).

Results and discussion

Synthesis and characterization of gold(I) and silver(I) trz complexes

We have previously reported the preparation of the precursor triarylated triazolium salt (**A,** Scheme 1) with a ferrocenyl substituent on the C4-position of the triazolium ring, and coordination of the trz ligand to rhodium(I) by generating the free carbene in situ with a non-nucleophilic potassium base.[29] However, using the same approach with Au(tht)Cl (tht = tetrahydrothiophene) resulted in intractable mixtures of the

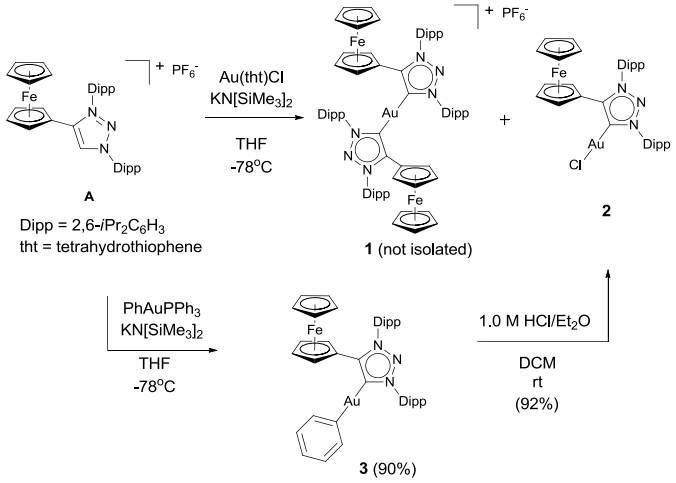

Scheme 1 Synthesis of the neutral gold(I) complexes **2** and **3**.

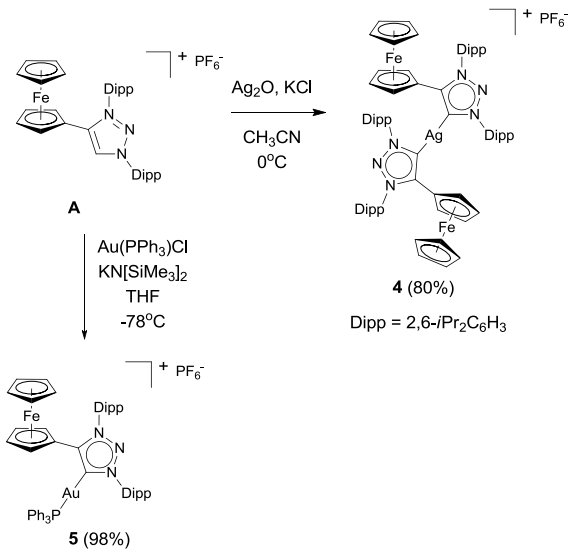

Scheme 2 Synthesis of the silver(I) bistriazolylidene complex **4** and the cationic gold(I) triphenylphosphine triazolylidene complex **5**.

target gold(I) chlorido trz complex **2**, as well as the gold(I) biscarbene complex **1** (Scheme 1, and Fig. S1 and S2 in the ESI). The carbene resonances are observed at 176.3 ppm and at 160.9 ppm for complex **1** and **2**, respectively, in the ^{13}C NMR spectrum.[30] The presence of an equilibrium between the neutral monocarbene and cationic biscarbene complexes of gold(I) has been argued,[31-33] and compromises the yield of the gold(I) trz chlorido complex. However, if the method of Bertrand et al. is employed, the gold(I) trz chlorido complex is formed exclusively from the hydrolysis of the gold(I) phenyl complex (**3**, Scheme 1), prepared by complexation of the in situ generated triazolylidene to the gold precursor $Au(PPh_3)Ph$.[30] Evidence for complex **3** formation is firstly, the disappearance of the acidic triazolium proton resonance in the ^{1}H NMR spectrum; and secondly, the appearance of the carbene carbon atom resonance at 183.1 ppm in the ^{13}C NMR spectrum. In contrast, the carbene chemical shift for the carbene carbon atom of **2** is observed upfield at 160.9 ppm.

The synthesis of the corresponding silver(I) trz chlorido complex was attempted for comparison to the gold(I) complexes for anti-tumoural activity. However only the silver(I) bis(triazolylidene) complex was isolated in high yield (**4**, Scheme 2). Both NMR and single crystal XRD analysis (*vide infra*) indicated the presence of the cationic biscarbene complex exclusively, and the formation of the neutral Ag(trz)Cl complex was not observed. Examples of isolated silver triazolylidenes are rare, as these compounds are employed as highly successful transmetalation intermediates.[22, 34] The carbene carbon atom of **4** resonates at 167.3 ppm, corresponding to other silver trz complexes reported.[35-37]

To compare the effect of a charged complex, which would have different solubility and lipophilic properties compared to the neutral gold chloride **2** in aqueous media, a cationic triphenylphosphine gold(I) complex, **5** was prepared by the

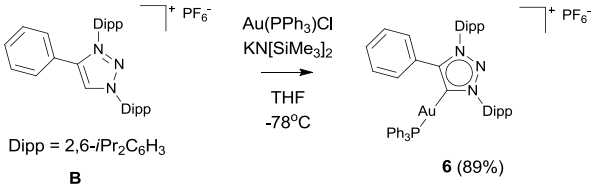

Scheme 3 The synthesis of the phenyl analogue, **6**, of the gold(I) triphenylphosphine complex, **5**.

facile deprotonation of **A** in the presence of $Au(PPh_3)Cl$.[38] The carbene carbon atom resonates at 176.2 ppm (J_{PC} = 120.5 Hz) in the ^{13}C NMR spectrum while the phosphine chemical shift appears as a singlet at 40.9 ppm in the ^{31}P NMR spectrum. A related gold(I) trz triphenylphosphine complex bearing mesityl wingtip groups on the triazolylidene ring, has been reported with a carbene chemical shift of 177 ppm (J_{PC} = 122 Hz).[39] This complex was prepared by reacting the Au(trz)Cl precursor with PPh_3 in the presence of a halide scavenger to afford the cationic $[Au(trz)PPh_3]^+$ complex in an alternative route.

To determine the effect of the ferrocenyl substituent with respect to the anticancer activity of the complexes, an analogue of **5** bearing a phenyl moiety on the C4-position of the triazolylidene ring, was synthesized from the known triazolium salt, **B** (Scheme 3).[40] Complex **6** is however unstable in solution over an extended period of time, and phosphine ligand dissociation occurs with resultant formation of the known cationic biscarbene analogue of **1**, as observed by NMR spectroscopy.[30] After 24 h, the carbene carbon resonances of both **6** (176.8 ppm) and the cationic biscarbene complex derived from precursor **B** (173.6 ppm) are seen in the ^{13}C NMR spectrum (see Fig. S14, ESI).[30] This ligand dissociation is not observed for the ferrocenyl analogue **5**, and demonstrates the enhanced stability of ferrocenyl trz gold(I) triphenylphosphine complex **5** compared to its non-ferrocenyl counterpart **6**.

Single crystal X-ray diffraction analysis.

Crystals of **2**, **3** and **4** (Fig. 2) were obtained from a solution of $CDCl_3$ by slow evaporation. From the single crystal X-ray diffraction studies of **2**, the Au-$C_{carbene}$ bond length was observed to be 1.981(3) Å, which is comparable both to the reported diarylated triazolylidene gold(I) chlorido Au-$C_{carbene}$ bond length

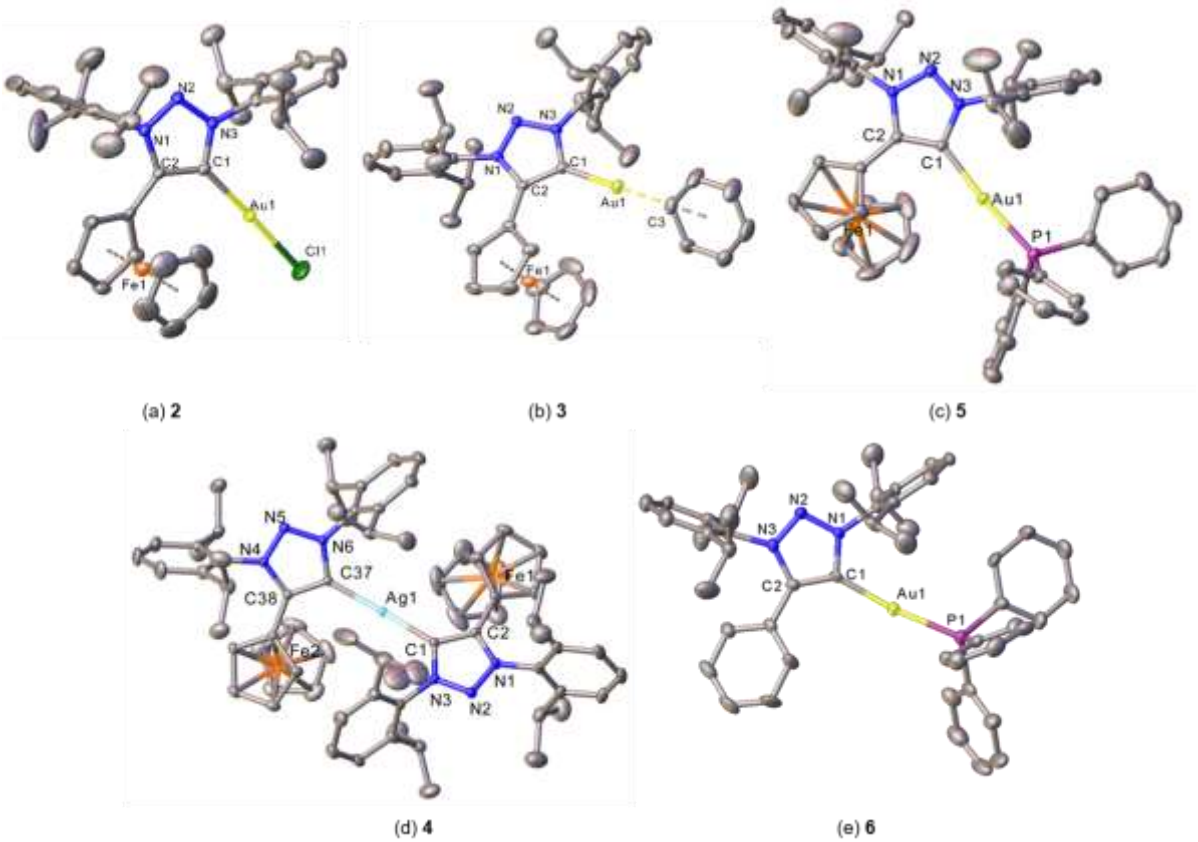

Fig. 2 Molecular structures of triazolylidene gold(I) complexes (a) **2**, (b) **3,** (c) **5**, (d) **4** and (e) **6** showing 50% probability ellipsoids and partial atom-numbering scheme. Selected bond lengths (Å) and angles (°) for **2**: Au1–C1 1.981(3); Au1-Cl1 2.2739(10); C1-Au1-Cl1 177.82(10); C2-C1-N3 103.1(3); for **3**: Au1–C1 2.024(2); Au1-C3 2.2040(2); C1-Au1-C3 177.81(9); C2-C1-N3 102.58(17); for **4**: Ag1–C1 2.0759(13); Ag1-C37 2.0790(13); C1-Ag1-C37 170.15(5); C2-C1-N3 102.06(11); C38-C37-N6 102.16(11).; for **5**: Au1–C1 2.045(19); Au1-P1 2.2834(5); C1-Au1-P1 175.47(6); C2-C1-N3 103.01(16); or **6**: Au1–C1 2.040(7); Au1-P1 2.278(2); C1-Au1-P1 174.6(2); C2-C1-N1 103.9(6). Hydrogens and PF_6^- counterions of **4**–**6**, are omitted for clarity.

Journal Name

ARTICLE

of 1.991(6) Å,[30] and to the ferrocenyl N1-alkylated triazolylidene gold(I) complex Au-$C_{carbene}$ bond length reported by Sarkar et al. as 1.982(2) Å;[41] falling well within the range of other Au-$C_{carbene}$ bond lengths reported for N1-alkylated gold(I) trz chlorido complexes (1.980–1.993 Å).[39] The Au-Cl bond length of 2.274(10) Å for **2** is similar to that of the other diarylated triazolylidene gold(I) chlorido complex reported (2.2761(17) Å),[30] but shorter than the corresponding Au-Cl bond lengths of N1-alkylated analogues (2.282–2.290 Å), indicating a decrease in the *trans* influence observed for the diarylated triazolylidene as compared to the N1-alkylated analogues.[39]

The Au-$C_{carbene}$ bond length of complex **3** (2.024(2) Å) is significantly longer, demonstrating the pronounced *trans* influence of the phenyl ligand on the triazolylidene, compared to the chlorido ligand. The average Ag-$C_{carbene}$ bond length of **4** (2.080(13) Å) corresponds well to other reported Ag-$C_{carbene}$ bond lengths ranging between 2.075 – 2.113 Å.[35-37] Significant deviation from linearity is found for the $C_{carbene}$-Ag-$C_{carbene}$ bond angle of 170.15(5)°; more than that reported for other silver bis(triazolylidene) complexes (177.9°–173.9°); presumably due to the steric bulk of the triarylated triazolylidene derived from **A**. [35-37] Crystals of **5** and **6** (Fig. 2) were grown from a concentrated dichloromethane (DCM) solution layered with toluene at room temperature. The Au-$C_{carbene}$ bond lengths of the heterobimetallic **5** and monometallic **6** (2.045(19) Å and 2.040(7) Å, respectively), and the Au-P bond lengths (2.283(5) Å and 2.278(2) Å, respectively), are nearly equivalent, as are the nearly linear $C_{carbene}$-Au-P bond angles of both **5** (175.47(6) °) and **6** (174.6(2) °).

As expected, the stronger *trans* influence of the triphenylphosphine co-ligand in complex **5**, results in the longest Au-$C_{carbene}$ bond length for the series of complexes derived from precursor triazolium salt **A** (**5** (2.045(19) Å) > **3** (2.024(2) Å) > **2** (1.981(3) Å)).

Cyclic voltammetry

The effect of the gold(I) coordination on the redox-activity of the ferrocenyl substituent of **A** was evaluated by cyclic voltammetry experiments on complexes **2** and **5** (Table 1). We have previously reported the redox potential of the Fe^{II}/Fe^{III} pair (0.3 V) for the triazolium salt **A**.[29] No redox event associated with the gold metal center was observed, consistent also with prior electrochemistry reports on gold(I) ferrocenyl triazolylidene complexes.[42,43] Both complexes only have one redox event on both the CV timescale and in the solvent window, namely the oxidation and reduction of the ferrocenyl substituent (See Fig. S15, ESI).

For complex **2**, Fe^{II} oxidation occurs at a lower oxidizing potential (145 mV, Table 1), than for the cationic **5** (298 mV), due to the electrostatic effect. As expected, dative covalent bonding of the trz to gold(I) lowers the potential of the Fe^{II}/Fe^{III} redox couple as observed in the difference of $E^{o'}$ between triazolium **A** (0.3 V) and complex **5** (0.22 V).

Table 1 Cyclic voltammetry (CV) data for the $Fe^{II/III}$ redox couple observed for complexes **2** and **5** vs. the Ag/Ag^+ couple, using the redox couple $[Fe(\eta^5\text{-}C_5Me_5)_2]^{+1/0}$ as the internal standard in CH_2Cl_2

Complex	2	5
E_{pa} (V)	0.145	0.298
E_{pc} (V)	0.044	0.137
$E^{o'}$ (V)	0.095	0.217
ΔE_p (V)	0.100	0.160
i_{pc}/i_{pa}	1.00	1.83

Stability studies in DMSO

The common use of dimethylsulfoxide (DMSO) stock solutions for biological assays and *in vitro* studies of metal complexes has the drawback of possible ligand dissociation due to the competing nucleophilic nature of the solvent DMSO.[44] For this reason, before evaluating the therapeutic profile of the synthesized complexes, we investigated the stability of the neutral complex **2** and cationic complex **5**, as representative examples of the series of complexes. Complexes **2** and **5** were dissolved in solvent 1:1 d_6-DMSO:H_2O, and the ^1H NMR spectra of the solutions were monitored at room temperature (298 K) at different time intervals (see Fig. S16 and S17, ESI). No changes in the spectra were observed during the course of this experiment, and both **2** and **5** was found to be stable in aqueous solution and d_6-DMSO for an extended period of time. In addition, HRMS was also employed as a tool to monitor stability of **5**. The presence of the molecular ion peak ($[M]^+$ = 1032.3390) as the major fragment ion was observed for a solution of **5** dissolved in DMSO for 5 days, to confirm the NMR stability tests (see Fig. S18, ESI).

Anticancer properties of gold complexes

Preliminary cytotoxicity studies of the precursor triazolium salts **A** and **B**, and their corresponding gold(I) complexes (neutral, **2**; and cationic, **5**, **6**) and silver(I) complex **4**, were conducted to evaluate their anticancer activity against the lung cancer cell lines A549 and H1975 as well as the human embryonic kidney cell line (HEK-293). The latter was employed

as a non-cancer cell model. In order to identify active ligand precursors and their complexes, cancer cells were exposed to concentrations of 50 µM and 5 µM for 48 hours (Fig. S19 and S20, ESI) and the percentage cell survival was determined using the MTT assay.[45] Only **5** was found to completely inhibit the growth of both the cancer cell lines at the lower concentration (5 µM). Further evaluation of **5** to determine its 50% inhibitory concentration value (IC_{50}) indicated potent activity with IC_{50} values of 0.89 and 0.23 µM against A549 and

Table 2 IC_{50} values of **5** against cancer and non-cancer cell lines ± standard deviation

Cell line	IC_{50} (µM)
A549	0.89±0.08
H1975	0.23±0.045
HEK-293	5.43±0.28

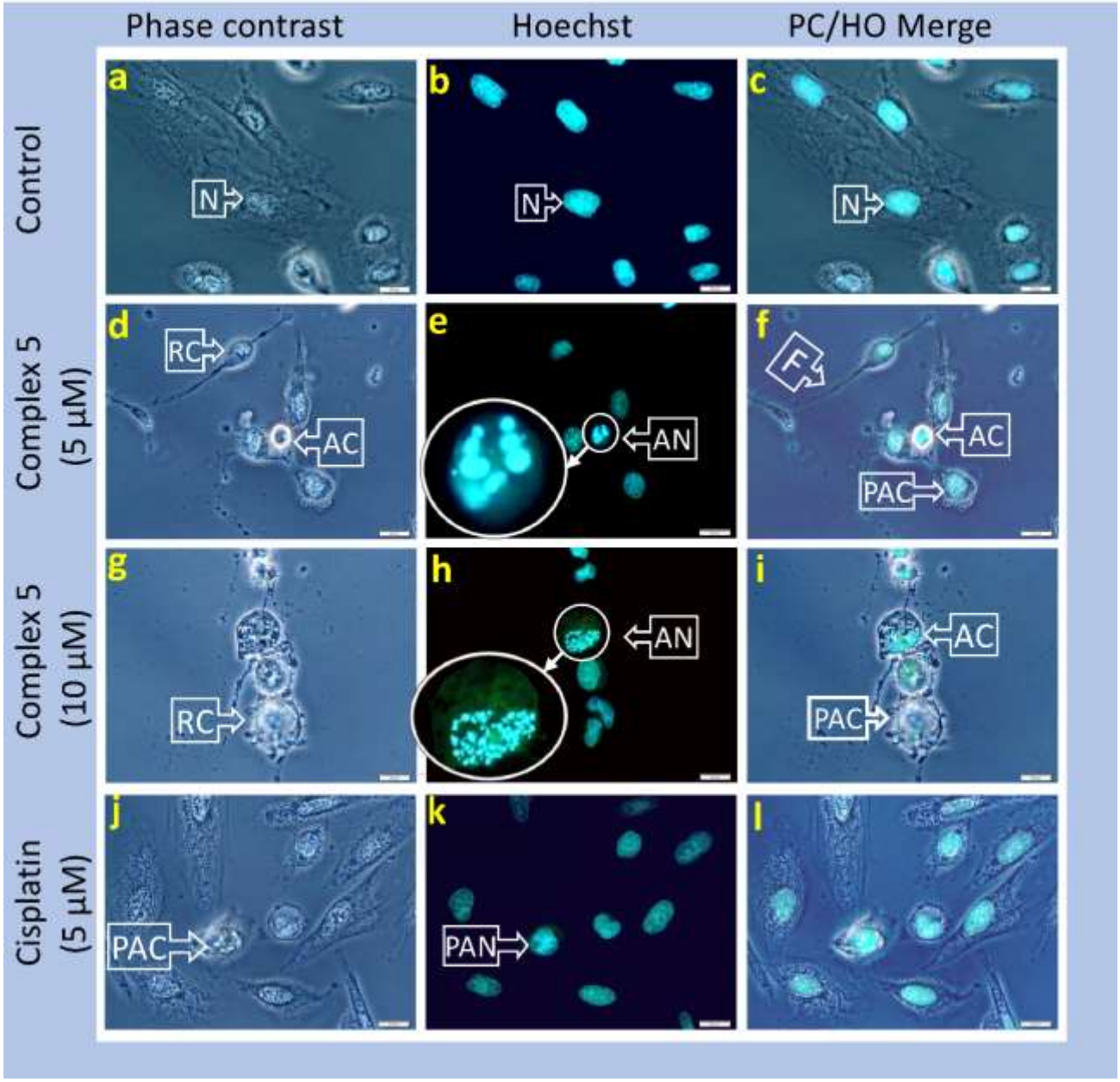

Fig. 3 H1975 lung cancer cells undergo apoptotic cell death when treated with gold complex **5.** H1975 cells were exposed to complex **5** at 5 and 10 µM concentrations for 18 hours. Staining of live unfixed cells with ethidium bromide and Hoechst dye showed the absence of necrosis and the presence of apoptotic nuclei. Cells were viewed under a 400X magnification with an Olympus BX41 epifluorescence microscope and images were captured with an Olympus DP72 digital camera and processed using the CellSens software package. Scalebar: 20 microns. Legend: N=nucleus, AC=apoptotic cell, AN= apoptotic nucleus, PAC= preapoptotic cell, PAN= preapoptotic nucleus, RC= rounded cell, F=filopodia

H1975 cells. These initial experiments demonstrate the efficacy of **5** as was the case with the related heterometallic gold ferrocenyl complexes reported by Arambula et al.[15] and Casini et al.,[16] in contrast to previously reported, but less active, gold trz complexes.[27] Direct comparison is, however, not possible due to different incubation times and assay

conditions employed. Moreover, **5** displayed only modest activity against the HEK-293 cells with an IC_{50} value of 5.43 µM, with one order of magnitude difference compared to the cancer cell lines, demonstrating limited selectivity.

Fluorescent microscopy studies with the vital dyes Hoechst 3342 (HO), ethidium bromide (EtBr) and acridine orange (AO),[46, 47] indicated that **5** induces apoptotic cell death in H1975 cells, when cells were exposed to 5 µM and 10 µM for 18 hours (Fig. 3). Exposure of H1975 cells to complex **5** shows that the majority of cells rounded up and was partially attached to the growth surface, by the formation of filopodia

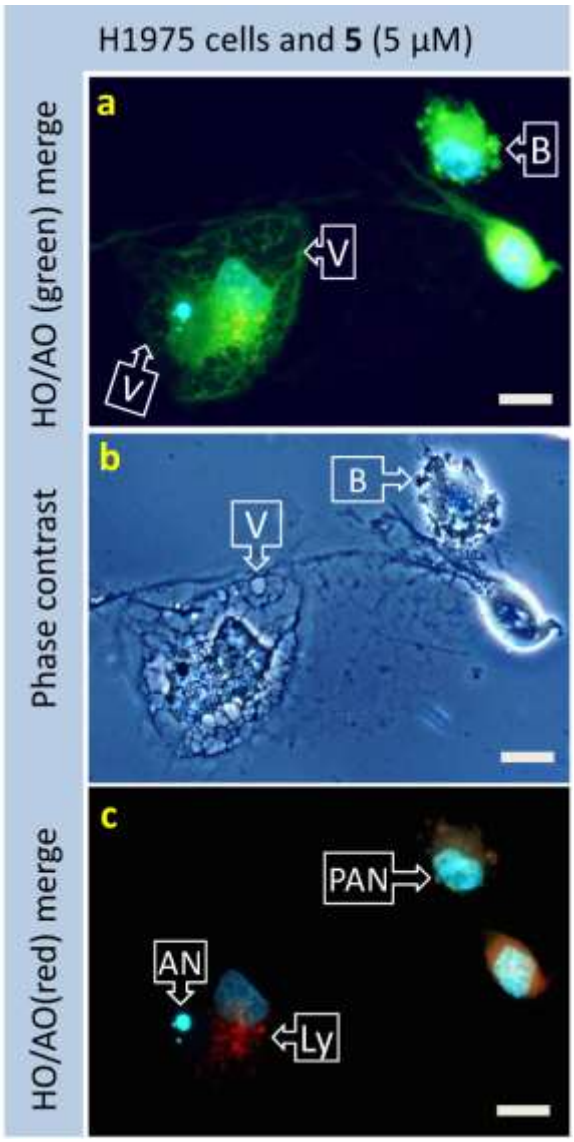

Fig. 4 Gold complex **5** induces vacuole formation in H1975 lung cancer cells. H1975 cells were exposed to complex **5** at a 5 µM concentration for 18 hours. Microscopic evaluation of cell morphology indicates the presence of numerous cytoplasmic vacuoles in cells that remained attached to the growth surface, the presence of lysosomes and cell membrane blebbing. Scalebar: 20 microns. Legend: V = vacuole, B = Blebbing, AN = apoptotic nucleus, PAN = preapoptotic nucleus, Ly = lysosomes, F = filopodia.

and more importantly, the formation of apoptotic nuclei as seen in Fig. 3, panels e, f, h, and i. Compared to non-apoptotic nuclei, apoptotic nuclei display a typical multiple globular pattern combined with an increased fluorescence signal. Cisplatin was used as a positive control in the preliminary morphology studies. In contrast with **5**, cells treated with 5 µM of freshly prepared cisplatin shows minimal effects, the cytoplasm had a more granular appearance but the majority of the cells remained attached to the growth surface and displayed a normal morphology. Only one cell appears to be in a pre-apoptotic state with condensed nuclear material. (Fig 3 panels j, k, l). This is an encouraging observation since cisplatin is widely used in the treatment of metastatic lung cancer.

Cells treated with **5** showed the formation of numerous cytoplasmic vacuoles before they detach from the growth surface (Fig. 4 panel a, b). Vacuoles are not clearly visible once the cells have rounded up and started to detach from the growth surface (Fig. 4 panels a and b). Vacuole formation is an indication of cell stress and frequently precedes stress-induced apoptosis or autophagy. Acridine orange indicates the formation of lysosomes which stains red, and which is considered to be a marker for cell stress and a preliminary indicator for autophagic cell death (Fig 4, panel c).[48] Blebbing of cell membranes, another apoptotic feature, was visible on the partially detached cells and is indicated by arrow B in Fig 4 (panels a and b). In addition, no staining of nuclei with ethidium bromide was observed which indicates that despite extensive morphological changes, the cell membranes remained intact. In comparison, when A549 cells were exposed to 5 µM of **5** for 18 hrs, no clear indication of apoptosis was observed (see ESI, Fig. S21). This is consistent with the higher IC_{50} value of A549; and treatment of A549 with higher concentration of **5** may well induce apoptosis, as the cells did show changes to the basic cellular and nuclear morphology.

Conclusions

A series of gold(I) 4-ferrocenyl-1,2,3-triazol-5-ylidene complexes were prepared and spectroscopically and structurally characterised, including neutral and cationic derivatives (**2**–**3**, **5**). In addition, a monometallic analogue bearing a phenyl triazolylidene (**6**) instead of the ferrocenyl trz, as well as the silver(I) bis(trz) (**4**), were also prepared. Coordination of the redox-active ferrocenyl trz ligand to a Au(I) centre results in an increase of the oxidation potential of the $Fe^{II/III}$ couple, compared to the corresponding precursor triazolium salt **A**. In addition, the cationic triphenylphosphine gold(I) complex **5** was found to be stable in aqueous media and in dimethylsulfoxide solutions over an extended period of time. The effect of (i) the heterobimetallic complexes **2**–**5** in comparison to the monometallic complex **6** and precursor **A**; (ii) cationic (**5**) vs. neutral (**2**) gold(I) complexes; and (iii) silver(I) (**4**) vs gold(I) (**5**, **6**) metal centra, was investigated in a preliminary study on the cytotoxic activity of the range of complexes. It was found that the most potent potential

anticancer agent was the heterobimetallic, cationic complex **5**, while microscopy studies indicated apoptotic cell death as a result of treatment with **5**. The study is indicative of the fact that both metal centres (Au(I) and Fe(II)), as well as the cationic nature of the compound, are required for improved activity against cancer cells. Future studies are in progress to evaluate the ROS mediated pathway of cell death in different cancer cell lines.

Experimental Section

General Considerations

All air and moisture sensitive synthetic procedures were performed under a N_2 (g) or Ar (g) atmosphere using standard Schlenk techniques. All solvents were purified and distilled over Na (s) (hexane, diethyl ether, benzene and tetrahydrofuran (THF)) or CaH_2 (dichloromethane and acetonitrile) under N_2 (g) atmosphere. Triazolium salts, **A**[29] and **B**[40] and metal precursors, Au(tht)Cl,[49] $Au(PPh_3)Cl$[50] and $Au(PPh_3)Ph$[51] were synthesized according to previously reported literature methods. All other reagents were commercially available and used without any purification thereof. Air sensitive solids were stored and handled in a Purelab HE glovebox. A Bruker AVANCE III 300.12 MHz or 400.21 MHz spectrometer was used for NMR experiments. Chemical shifts are reported as δ (in ppm) and reported relative to the deuterated solvent signal: For $CDCl_3$, δH at 7.26 ppm, and δC at 77.16 ppm, respectively. The ^{31}P {1H} NMR spectra were referenced to the deuterated lock solvent, which had been referenced to 85% H_3PO_4. The NMR assignment of each complex follows the numbering scheme indicated in the ESI. Mass spectral analyses were performed on a Waters Synapt G2 HDMS by direct infusion at 5 µL/min with positive electron spray as the ionization technique for 3 minutes. The m/z values were measured in the range of 50-2000 in acetonitrile. Prior to analysis, sodium formate (5 mM) was used to calibrate the instrument in resolution mode. Elemental analyses were carried out using a Thermo Flash 1112 Series CHNS-O Analyzer. Melting points were measured with a Stuart SMP10 melting point apparatus. Electrochemical studies were carried out using a three-electrode cell. The reference electrode was a non-aqueous Ag/Ag^+ electrode, separated by the test solution by a frit with fine porosity. Glassy carbon disc (3.0 mm diameter) was the working electrode and the counter electrode was a platinum wire. Measurements were done on a Metrohm µAutolab type III potentiostat, using NOVA 2.0 electrochemistry software at scan rates of 100 $mV.s^{-1}$. To a deoxygenated solution of 0.1 M $[N^nBu_4][PF_6]$ (supporting electrolyte) in HPLC grade $CH2Cl_2$, the test compound (1.0 mM) and the internal standard, $[Fe(\eta^5\text{-}C_5(CH_3)_5)_2]$ was added. Under these conditions, the redox couple for $[Fe(\eta^5\text{-}C_5H_5)_2]^{0/+1}$ is -0.54 V.

***In vitro* anticancer activity**:

The cytotoxic effects of the compounds were evaluated on the lung cancer cell lines, A549 and H1975 and the normal HEK-293 cell line by the MTT assay.[45] Stock solutions (10 mM) were prepared in DMSO. Test concentrations for the MTT assay were prepared by diluting the compounds in cell culture medium with the final DMSO concentration in the medium never exceeding 0.01%. Cells were seeded in a 96 well plate and allowed to adhere overnight before the addition of test compounds. Cells were exposed to the test compounds for 48 h in a humified incubator at 37°C and 5% CO_2. At 46 h, 40 µL of MTT (5mg/ml) was added to each well and the plates incubated for 2 hours at 37°C. This was followed by centrifugation for 5 min and aspiration of the growth media. The formazan crystals were dissolved by the addition of 200 µL of DMSO followed by shaking of the plate for 5 min at 1000 rpms. The absorbances of each well were measured in a Lab Systems iEMS microplate reader at 540 nm and a reference wavelength of 690 nm. All data points of each experiment were obtained in quadruplicates and at least three independent experiments were performed. The percentage of cell viability was calculated by expressing the absorbance of the treated cells as a percentage of untreated control cells. IC_{50} values were obtained by using non-linear regression analysis of GraphPad Prizm version 7 software package.

Cell Morphology

The A549 and H1975 cells were grown on sterile glass coverslips which were placed in 6 well culture plates. Cells were seeded at a density of 50 000 cells per coverslip and allowed to adhere overnight before the start of the treatment. Media was removed the following day and replaced with culture medium containing the test compounds. Cells were incubated for 18 h at 37 °C in a humidified incubator supplemented with 5% CO_2. The cells were gently washed with phosphate buffered saline (PBS) and then incubated with 500 µl of the vital dye mix for 30 minutes in the dark. The vital dye mixture contained acridine orange (10 µg/mL), ethidium bromide (10 µg/mL) and Hoechst (5 µg/mL) in PBS. The coverslips were then washed with PBS and placed cell side downwards on a microscopic slide containing a drop of Fluoromount mounting media (Sigma). The cells were viewed with an Olympus BX41 epifluorescent microscope 400 times magnification using appropriate filters for acridine orange, ethidium bromide, and Hoechst. Images were captured in colour mode with a DP72 digital camera with an ISO setting of 400 and a fixed exposure time for each fluorochrome. Captured images were adjusted for brightness and contrast where required and phase contrast images were merged with Hoechst images using the Olympus CellSens software package.

Synthesis of Complexes 1–6.

Bis(1,3-bis(2,6-diisopropylphenyl)-4-ferrocenyl-1,2,3-triazol-5-ylidene) gold(I) hexafluorophosphate, 1. A solution of Au(tht)Cl (0.07 g, 0.21 mmol) in THF was added to a solution of triazolium salt, **A** (0.15 g, 0.21 mmol) and $KN[SiMe_3]_2$ (0.07 g, 0.33 mmol) in THF at -78 °C. The reaction proceeded overnight whilst warming to room temperature. The solvent was

evaporated, and the residue was washed with ether, followed by extraction with DCM affording a mixture of **1** and **2**, as a reddish brown solid. For **1**: ^{1}H NMR (400 MHz, $CDCl_3$) δ 7.69 (dt, *J* = 15.9, 7.8 Hz, 4H, Dipp-CH, H-1), 7.44 (d, *J* = 7.9 Hz, 4H, Dipp-CH, H-2), 7.40 (d, *J* = 7.9 Hz, 4H, Dipp-CH, H-2), 4.27 (m, 2H, Fc-CH, H-3), 4.13 (t, *J* = 1.9, 4H, Fc-CH, H-3), 4.03 (s, 9H, Fc-CH, H-3), 3.87 (m, 3H, Fc-CH, H-3), 2.58 (p, *J* = 7.1 Hz, 4H, Dipp(iso)-CH, H-4), 2.40–2.25 (m, 4H, Dipp(iso)-CH, H-4), 1.40 (d, *J* = 6.8 Hz, 9H, Dipp(iso)-CH_3, H-5), 1.25 (d, *J* = 6.8 Hz, 12H, Dipp(iso)-CH_3, H-5), 1.15–1.12 (m, 27H, Dipp(iso)-CH_3, H-5). ^{13}C {^{1}H} NMR (75 MHz, $CDCl_3$) δ 173.26 ($C_{carbene}$, C-1), 151.14 (trz-C_q, C-2), 145.1 (Dipp-C_q, C-3), 132.8 (Dipp-C_q, C-4), 132.6 (Dipp-C_q, C-4), 131.2 (Dipp-CH, C-5), 129.2 (Dipp-CH, C-5), 128.5 (Dipp-CH, C-5), 128.4 (Dipp-CH, C-5), 125.4 (Dipp-CH, C-6), 125.2 (Dipp-CH, C-6), 124.8 (Dipp-CH, C-6), 71.2 (Fc-CH, C-7), 70.6 (Fc-CH, C-7), 69.6 (Fc-C_q, C-8), 68.4 (Fc-CH, C-7), 29.5 (Dipp(iso)-CH, C-9), 29.4 (Dipp(iso)-CH, C-9), 25.2 (Dipp(iso)-CH_3, C-10), 24.6 (Dipp(iso)-CH_3, C-10), 24.4 (Dipp(iso)-CH_3, C-10), 23.0 (Dipp(iso)-CH_3, C-10). ESI-HRMS (15 V, positive mode, m/z): calcd. for $[M]^+$: 1343.5280 Found: 1343.5278.

1,3-bis(2,6-diisopropylphenyl)-4-ferrocenyl-1,2,3-triazol-5-ylidene gold(I) chloride, 2. Complex **3** (0.52 g, 0.62 mmol) was suspended in DCM and an excess of 1.0 M HCl in diethyl ether (3.8 mL) was added and stirred for one hour. The solvent was evaporated affording **2** as a yellow brown solid in near-quantitative yield. Yield: 0.45 g (92%). M.p. 145–149 °C. ^{1}H NMR (400 MHz, $CDCl_3$) δ 7.57 (m, 2H, dipp-CH, H-1), 7.34 (t, *J* = 7.8 Hz, 4H, Dipp-CH, H-2), 4.61 (br s, 2H, Fc-CH, H-3), 4.26 (br s, 7H, Fc-CH, H-4), 2.49 (dt, *J* = 13.4, 6.7 Hz, 2H, Dipp(iso)-CH, H-5), 2.37 (dd, *J* = 12.1, 5.8 Hz, 2H, Dipp(iso)-CH, H-5), 1.46 (d, *J* = 6.8 Hz, 6H, Dipp(iso)-CH_3, H-6), 1.16 (m, 18H, Dipp(iso)-CH_3, H-6). ^{13}C {^{1}H} NMR (75 MHz, $CDCl_3$) δ 160.9 ($C_{carbene}$, C-1), 148.7 (trz-C_q, C-2), 145.4 (Dipp-C_q, C-3), 144.9 (Dipp-C_q, C-3), 135.3 (Dipp-C_q, C-4), 132.3 (Dipp-C_q, C-4), 131.5 (Dipp-CH, C-5), 131.3 (Dipp-CH, C-5), 124.7 (Dipp-CH, C-6), 124.3 (Dipp-CH, C-6), 70.7 (Fc-CH, C-7), 70.1 (Fc-CH, C-8), 69.5 (Fc-C_q, C-10), 69.3 (Fc-CH, C-9), 29.0 (Dipp(iso)-CH, C-11), 24.9 (Dipp(iso)-CH_3, C-12), 24.5 (Dipp(iso)-CH_3, C-12), 24.2 (Dipp(iso)-CH_3, C-12), 22.9 (Dipp(iso)-CH_3, C-12). Anal. Calcd. for $C_{36}H_{43}N_3FeAuCl$ (1 eq H_2O): C 52.48, H 5.26, N 5.10. Found: C 52.73, H 4.92, N 4.70. ESI-HRMS (15 V, positive mode, m/z): calcd. for $[M+H+NH_4]^{2+}$: 824.2582. Found: 824.2578.

1,3-bis(2,6-diisopropylphenyl)-4-ferrocenyl-1,2,3-triazol-5-ylidene gold(I) phenyl, 3. The synthesis of complex **3** was accomplished by following a previously reported procedure.[30] a solution of $Au(PPh_3)Ph$ (0.41 g, 0.76 mmol) in THF at -30 °C was added dropwise to a solution of **A** (0.5 g, 0.69 mmol) and $KN[SiMe_3]_2$ (0.14 g, 0.76 mmol) in THF at -78 °C. The reaction was left to stir overnight, while reaching room temperature. After the solvent was evaporated, the residue was washed with hexane and the product was extracted with toluene, as a yellow solid in quantitative yield. Yield: 0.53 g (90%). ^{1}H NMR (400 MHz, $CDCl_3$) δ 7.59 (t, *J* = 7.8 Hz, 1H, Dipp-CH, H-1), 7.53 (m, 1H, Dipp-CH, H-1), 7.48 (dd, *J* = 7.6, 1.3 Hz, 2H, Dipp-CH, H-2), 7.34 (dd, *J* = 11.9, 7.9 Hz, 4H. Ph-CH, H-3), 7.18 (t, *J* = 7.5 Hz, 2H, Dipp-CH, H-2), 6.98 (dd, *J* = 10.3, 4.4 Hz, 1H, Ph-CH, H-4), 4.73 (m, 2H, Fc-CH, H-5), 4.29 (m, 5H, Fc-CH, H-6), 4.23 (m, 2H, Fc-CH, H-7), 2.61 (dt, *J* = 13.7, 6.9 Hz, 2H, Dipp(iso)-CH, H-8), 2.44 (dt, *J* = 13.6, 6.8 Hz, 2H, Dipp(iso)-CH, H-8), 1.52 (d, *J* = 6.8 Hz, 6H, Dipp(iso)-CH_3, H-9), 1.21 (d, *J* = 6.9 Hz, 6H, Dipp(iso)-CH_3, H-9), 1.16 (d, *J* = 6.8 Hz, 12H, Dipp(iso)-CH_3, H-9). ^{13}C {^{1}H} NMR (75 MHz, $CDCl_3$) δ 183.1 ($C_{carbene}$, C-1), 172.7 (Au-PhC_q, C-2), 149.5 (trz-C_q, C-3), 145.7 (Dipp-C_q, C-4), 145.0 (Dipp-C_q, C-4), 140.9 (Ph-CH, C-5), 136.0 (Ph-CH, C-6), 131.9 (Dipp-C_q, C-7), 131.0 (Dipp-C_q, C-7), 127.1 (Ph-CH, C-8), 124.7 (Dipp-CH, C-9), 124.4 (Dipp-CH, C-10), 124.1 (Dipp-CH, C-9), 71.1 (Fc-CH, C-11), 70.8 (Fc-CH, C-12), 69.9 (Fc-C_q, C-13), 68.5 (Fc-CH, C-14), 29.2 (Dipp(iso)-CH, C-15), 25.0 (Dipp(iso)-CH_3, C-16), 24.6 (Dipp(iso)-CH_3, C-16), 24.3 (Dipp(iso)-CH_3, C-16), 23.0 (Dipp(iso)-CH_3, C-16). ESI-HRMS (15 V, positive mode, m/z): calcd for $[M\text{-}C_6H_5+ACN]^+$: 811.2732. Found: 811.2764.

Bis(1,3-bis(2,6-diisopropylphenyl)-4-ferrocenyl-1,2,3-triazol-5-ylidene) silver(I) hexafluorophosphate, 4. Triazolium salt, **A** (0.2 g, 0.28 mmol), Ag_2O (0.26 g, 1.11 mmol) and KCl (0.12 g, 1.67 mmol) was added to a purged Schlenk tube in the absence of light and cooled down to 0 °C. Cooled degassed CH_3CN was added, and the reaction was left to stir for 30 minutes, after which it was permitted to stir overnight at room temperature. After evaporation of the solvent, the residue was washed with toluene, and the product was extracted with DCM, affording **4** as a light orange powder. Yield: 0.3 g (80%). M.p. 252–258 °C (decomp.). ^{1}H NMR (400 MHz, $CDCl_3$) δ 7.74 (t, *J* = 7.8 Hz, 1H, Dipp-CH, H-1), 7.67 (t, *J* = 7.8, 1H, Dipp-CH, H-1), 7.47 (d, *J* = 7.9 Hz, 2H. Dipp-CH, H-2), 7.41 (d, *J* = 7.9 Hz, 2H, Dipp-CH, H-2), 4.17 (m, 2H, Fc-CH, H-3), 4.04 (s, 4H, Fc-CH, H-4), 3.83 (m, 2H, Fc-CH, H-5), 2.54 (dt, *J* = 13.7, 6.7 Hz, 2H, Dipp(iso)-CH, H-6), 2.29 (dt, *J* = 14.1, 7.0 Hz, 2H, Dipp(iso)-CH, H-6), 1.34 (d, *J* = 6.8 Hz, 6H, Dipp(iso)-CH_3, H-7), 1.26 (d, *J* = 6.9 Hz, 6H, Dipp(iso)-CH_3, H-7), 1.16 (d, *J* = 6.7 Hz, 4.1 Hz, 12H, Dipp(iso)-CH_3, H-7). ^{13}C NMR (75 MHz, $CDCl_3$) δ 167.3 (dd, J_{AgC} = 181.2, 13.1 Hz, $C_{carbene}$, C-1), 151.6 (trz-C_q, C-2), 151.5 (trz-C_q, C-2), 145.2 (Dipp-C_q, C-3), 145.0 (Dipp-C_q, C-3), 136.0 (Dipp-C_q, C-4), 132.7 (Dipp-C_q, C-4), 132.32 (Dipp-CH, C-5), 131.0 (Dipp-CH, C-5), 125.0 (Dipp-CH, C-6), 124.8 (Dipp-CH, C-6), 71.1 (Fc-CH, C-7), 70.5 (Fc-CH, C-8), 69.5 (Fc-C_q, C-9), 68.6 (Fc-CH, C-10), 29.4 (Dipp(iso)-CH, C-11), 29.23 (Dipp(iso)-CH, C-11), 25.1 (Dipp(iso)-CH_3, C-12), 24.6 (Dipp(iso)-CH_3, C-12), 24.3 (Dipp(iso)-CH_3, C-12), 23.0 (Dipp(iso)-CH_3, C-12). ^{31}P {^{1}H} NMR (121 MHz, $CDCl_3$) δ -144.26 (dt, *J* = 712.3 Hz, 1424.3 Hz, PF_6). ^{19}F {^{1}H} NMR (282 MHz, $CDCl_3$) δ -73.93 (d, *J* = 712.2 Hz, PF_6). Anal. Calcd. for $C_{72}H_{86}N_6Fe_2AgPF_6$ (3 eq $(CH_3)_2CO$): C 61.80, H 6.66, N 5.34. Found: C 62.22, H 6.50, N 5.13. ESI-HRMS (15 V, positive mode, m/z): calcd. for $[M]^+$: 1253.4663. Found: 1253.4719.

1,3-bis(2,6-diisopropylphenyl)-4-ferrocenyl-1,2,3-triazol-5-ylidene gold(I) triphenylphosphine, 5. A solution of $Au(PPh_3)Cl$ (0.08 g, 0.15 mmol) in THF was added to a solution of triazolium salt, **A** (0.1 g, 0.14 mmol) and $KN[SiMe_3]_2$ (0.03 g, 0.15 mmol) in THF at -78 °C. The reaction proceeded overnight whilst warming to room temperature. The solvent was evaporated, and the residue was washed with toluene, followed by extraction with DCM affording **5** as an orange solid in near-quantitative yield. Yield: 0.16 g (98%). M.p. 249–256 °C (decomp.). ^{1}H NMR (400 MHz, $CDCl_3$) δ 7.78 (t, *J* = 7.8, 1H,

Dipp-CH, H-1), 7.67 (t, *J* = 7.8, 1H, Dipp-CH, H-1), 7.60 (m, 3H, Ph-CH, H-2), 7.50 (t, *J* = 7.2, 6H, Ph-CH, H-3), 7.43 (dd, *J* = 12.5, 8.3 Hz, 4H, Dipp-CH, H-4), 7.32 (dd, *J* = 12.9, 7.4 Hz, 6H, Ph-CH, H-5), 4.39 (br s, 4H, Fc-CH, H-6), 3.99 (br s, 5H, Fc-CH, H-7), 2.47 (dt, *J* = 13.4, 6.7 Hz, 2H, Dipp(iso)-CH, H-8), 2.30 (dd, *J* = 13.5, 6.7 Hz, 2H, Dipp(iso)-CH, H-8), 1.28 (d, *J* = 6.8 Hz, 6H, Dipp(iso)-CH_3, H-9), 1.22 (d, *J* = 6.8 Hz, 6H, Dipp(iso)-CH_3, H-9), 1.16 (d, *J* = 6.8 Hz, 12H, Dipp(iso)-CH_3, H-9). ^{13}C {^1H} NMR (75 MHz, $CDCl_3$) δ 176.2 (d, J_{PC} = 120.5 Hz, $C_{carbene}$, C-1), 151.1 (d, *J* = 7.8 Hz, trz-C_q, C-2), 145.3 (Dipp-C_q, C-3), 145.2 (Dipp-C_q, C-3), 135.2 (Dipp-C_q, C-4), 133.9 (d, *J* = 13.6 Hz, Ph-CH, C-5), 132.9 (Dipp-C_q, C-6), 132.7 (Ph-CH, C-7), 132.3 (Dipp-CH, C-6), 130.7 (Dipp-C_q, C-4), 129.9 (d, *J* = 11.5 Hz, Ph-CH, C-8), 128.0 (d, *J* = 58.3 Hz, Ph-C_q, C-9), 125.1 (Dipp-CH, C-10), 124.8 (Dipp-CH, C-10), 71.3 (Fc-CH, C-11), 70.6 (Fc-CH, C-12), 69.5 (Fc-CH, C-13), 68.3 (Fc-C_q, C-14), 29.4 (Dipp(iso)-CH, C-15), 24.3 (Dipp(iso)-CH_3, C-15), 25.0 (Dipp(iso)-CH_3, C-16), 24.5 (Dipp(iso)-CH_3, C-16), 24.4 (Dipp(iso)-CH_3, C-16), 22.9 (Dipp(iso)-CH_3, C-16). ^{31}P {^1H} NMR (121 MHz, $CDCl_3$) δ 40.9 (s, Ph_3-P-Au), -144.27 (dt, *J* = 712.3 Hz, 1424.5 Hz, PF_6). ^{19}F {^1H} NMR (282 MHz, $CDCl_3$) δ -73.85 (d, *J* = 712.2 Hz, PF_6). Anal. Calcd for $C_{54}H_{58}N_3FeAuP_2F_6$ (6.5eq H_2O): C 50.05, H 4.51, N 3.24. Found: C 50.47, H 4.21, N 2.84. ESI-HRMS (15 V, positive mode, m/z): calcd. for $[M]^+$: 1032.3383. Found: 1032.3416.

1,3-bis(2,6-diisopropylphenyl)-4-phenyl-1,2,3-triazol-5-ylidene gold(I) triphenylphosphine, 6. A solution of $Au(PPh_3)Cl$ (0.09 g, 0.18 mmol) in THF was added to a solution of triazolium salt, **B** (0.1 g, 0.16 mmol) and $KN[SiMe_3]_2$ (0.04 g, 0.18 mmol) in THF at -78 °C, and reaction proceeded overnight while warming to room temperature. The solvent was evaporated, and the residue was washed with toluene, followed by extraction with DCM affording **6** as a white solid. Yield: 0.15 g (89%). M.p. 140–143 °C (decomp.). ^1H NMR (400 MHz, $CDCl_3$) δ 7.74–7.64 (m, 2H, Dipp-CH, H-1), 7.62–7.41 (m, 15H, ph-CH_{PPh3}, H-2), 7.40–7.36 (m, 2H, Ph-CH, H-3), 7.28 (br s, 3H, Ph-CH, H-3), 7.24–7.22 (m, 2H, Dipp-CH, H-4), 7.14–7.09 (m, 2H, Dipp-CH, H-4), 2.47 (dt, *J* = 12.9, 5.3 Hz, 1H, Dipp(iso)-CH, H-5), 2.31 (dt, *J* = 18.9, 7.6 Hz, 2H, Dipp(iso)-CH, H-5), 2.19 (m, 1H, Dipp(iso)-CH_3, H-5), 1.24 (d, *J* = 6.9 Hz, 3H, Dipp(iso)-CH_3, H-6), 1.21 (d, *J* = 5.9 Hz, 3H, Dipp(iso)-CH_3, H-6), 1.16 (d, *J* = 6.2 Hz, 3H, Dipp(iso)-CH_3, H-6), 1.13 (d, *J* = 6.3 Hz, 3H, Dipp(iso)-CH_3, H-6), 1.08 (t, *J* = 8.5 Hz, 6H, Dipp(iso)-CH_3, H-6), 1.02 (d, *J* = 6.1 Hz, 3H, Dipp(iso)-CH_3, H-6), 0.96 (d, *J* = 5.9 Hz, 3H, Dipp(iso)-CH_3, H-6). ^{13}C {^1H} NMR (75 MHz, $CDCl_3$) δ 176.8 (d, J_{PC} = 120.0 Hz, $C_{carbene}$, C-1), 150.3 (d, *J* = 7.7 Hz, trz-C_q, C-2), 145.3(4) (Dipp-C_q, C-3), 145.3 (Dipp-C_q, C-3), 134.9 (Dipp-C_q, C-4), 134.3 (d, *J* = 13.9 Hz, $PhCH_{PPh3}$, C-5), 134.0 (d, *J* = 13.8 Hz, $PhCH_{PPh3}$, C-5), 132.5 (d, *J* = 2.7 Hz, $PhCH_{PPh3}$, C6), 132.3(2), 132.3, 132.2 (all Dipp-CH, C7), 132.1(5) (d, *J* = 2.7 Hz, $PhCH_{PPh3}$, C6), 132.1 (d, *J* = 2.7 Hz, $PhCH_{PPh3}$, C6), 131.4 (Dipp-C_q, C-4), 130.25 (Ph-CH, C-8), 129.8 (d, *J* = 11.6 Hz, Ph-CH_{PPh3}, C-9), 129.4(3), 129.4, 129.9 (all Dipp-CH, C-10), 128.6 (d, *J* = 11.9 Hz, $PhCH_{PPh3}$, C9), 128.1 (d, *J* = 58.5 Hz, Ph-C_q, C-11) , 125.2 (Ph-CH, C-8), 125.1 (Ph-C_q, C-12), 124.8 (Ph-CH, C-18), 29.6 (Dipp(iso)-CH, C-15), 29.3 (Dipp(iso)-CH, C-15), 25.4 (Dipp(iso)-CH_3, C-15), 24.6 (Dipp(iso)-CH_3, C-16), 24.3 (Dipp(iso)-CH_3, C-16), 22.6 (Dipp(iso)-CH_3, C-16). ^{31}P {^1H} NMR (121 MHz, $CDCl_3$) δ 40.8 (s, Ph_3-P-Au), -144.27 (dt, J = 712.3 Hz, 1424.5 Hz, PF_6). ^{19}F {^1H} NMR (282 MHz, $CDCl_3$) δ -73.85 (d, *J* = 712.2 Hz, PF_6). ESI-HRMS (15 V, positive mode, m/z): calcd. for $[M]^+$: 924.37207. Found: 924.3737.

Conflicts of interest

There are no conflicts to declare.

Acknowledgements

DA and DIB acknowledge the National Research Foundation, South Africa (NRF 105529; NRF 100119), and Sasol Technology R&D Pty. Ltd. (South Africa) for financial support. SVK thanks WITS URC for a postdoctoral fellowship. LH gratefully acknowledges the financial support of the McGill Bequest to the Pharmacology Division.

References

Uncategorized References

1. V. Fernandez-Moreira and M. C. Gimeno, *Chem. - Eur. J.*, 2018, **24**, 3345-3353.
2. P. Govender, H. Lemmerhirt, A. T. Hutton, B. Therrien, P. J. Bednarski and G. S. Smith, *Organometallics*, 2014, **33**, 5535-5545.
3. B. T. Elie, Y. Pechenyy, F. Uddin and M. Contel, *JBIC, J. Biol. Inorg. Chem.*, 2018, **23**, 399-411.
4. D. Nieto, A. M. Gonzalez-Vadillo, S. Bruna, C. J. Pastor, C. Rios-Luci, L. G. Leon, J. M. Padron, C. Navarro-Ranninger and I. Cuadrado, *Dalton Trans.*, 2012, **41**, 432-441.
5. N. Lease, V. Vasilevski, M. Carreira, A. de Almeida, M. Sanau, P. Hirva, A. Casini and M. Contel, *J. Med. Chem.*, 2013, **56**, 5806-5818.
6. S. D. R. van and N. Metzler-Nolte, *Chem Rev*, 2004, **104**, 5931-5985.
7. G. Gasser, I. Ott and N. Metzler-Nolte, *J. Med. Chem.*, 2011, **54**, 3-25.
8. C. G. Hartinger, N. Metzler-Nolte and P. J. Dyson, *Organometallics*, 2012, **31**, 5677-5685.
9. M. Patra and G. Gasser, *Nature Reviews Chemistry*, 2017, **1**, 0066.
10. C. Ornelas, *New J. Chem.*, 2011, **35**, 1973-1985.
11. O. Dada, G. Sanchez-Sanz, M. Tacke and X. Zhu, *Tetrahedron Lett.*, 2018, **59**, 2904-2908.
12. J. Rieb, B. Dominelli, D. Mayer, C. Jandl, J. Drechsel, W. Heydenreuter, S. A. Sieber and F. E. Kuehn, *Dalton Trans.*, 2017, **46**, 2722-2735.
13. C. Schmidt, B. Karge, R. Misgeld, A. Prokop, R. Franke, M. Broenstrup and I. Ott, *Chem.Eur. J.*, 2017, **23**, 1869-1880.
14. C. Zhang, C. Hemmert, H. Gornitzka, O. Cuvillier, M. Zhang and R. W.-Y. Sun, *Chem.Med.Chem*, 2018, **13**, 1218-1229.
15. J. F. Arambula, R. McCall, K. J. Sidoran, D. Magda, N. A. Mitchell, C. W. Bielawski, V. M. Lynch, J. L. Sessler and K. Arumugam, *Chem. Sci.*, 2016, **7**, 1245-1256.
16. J. K. Muenzner, B. Biersack, A. Albrecht, T. Rehm, U. Lacher, W. Milius, A. Casini, J.-J. Zhang, I. Ott, V. Brabec, O. Stuchlikova, I. C. Andronache, L. Kaps, D. Schuppan and R. Schobert, *Chem.Eur. J.*, 2016, **22**, 18953-18962.

17. P. Mathew, A. Neels and M. Albrecht, *J. Am. Chem. Soc.*, 2008, **130**, 13534-13535.
18. K. F. Donnelly, A. Petronilho and M. Albrecht, *Chem. Commun* , 2013, **49**, 1145-1159.
19. L. Suntrup, S. Hohloch and B. Sarkar, *Chem.Eur. J.*, 2016, **22**, 18009-18018.
20. J. Lorkowski, P. Zak, M. Kubicki, C. Pietraszuk, D. Jedrzkiewicz and J. Ejfler, *New J. Chem.*, 2018, **42**, 10134-10141.
21. K. O. Marichev, S. A. Patil and A. Bugarin, *Tetrahedron*, 2018, **74**, 2523-2546.
22. A. Vivancos, C. Segarra and M. Albrecht, *Chem. Rev.*, 2018, DOI: 10.1021/acs.chemrev.8b00148, Ahead of Print.
23. Y. Liu, K. S. Kjaer, L. A. Fredin, P. Chabera, T. Harlang, S. E. Canton, S. Lidin, J. Zhang, R. Lomoth, K.-E. Bergquist, P. Persson, K. Waernmark and V. Sundstroem, *Chem.Eur. J.*, 2015, **21**, 3628-3639.
24. A. Baschieri, F. Monti, E. Matteucci, A. Mazzanti, A. Barbieri, N. Armaroli and L. Sambri, *Inorg. Chem.*, 2016, **55**, 7912-7919.
25. J. Soellner, M. Tenne, G. Wagenblast and T. Strassner, *Chem.Eur. J.*, 2016, **22**, 9914-9918.
26. B. Sarkar and L. Suntrup, *Angew. Chem., Int. Ed.*, 2017, **56**, 8938-8940.
27. S. Vanicek, M. Podewitz, J. Stubbe, D. Schulze, H. Kopacka, K. Wurst, T. Mueller, P. Lippmann, S. Haslinger, H. Schottenberger, K. R. Liedl, I. Ott, B. Sarkar and B. Bildstein, *Chem.Eur. J.*, 2018, **24**, 3742-3753.
28. K. J. Kilpin, S. Crot, T. Riedel, J. A. Kitchen and P. J. Dyson, *Dalton Trans.*, 2014, **43**, 1443-1448.
29. D. Aucamp, T. Witteler, F. Dielmann, S. Siangwata, D. C. Liles, G. S. Smith and D. I. Bezuidenhout, *Eur. J. Inorg. Chem.*, 2017, **2017**, 1227-1236.
30. D. R. Tolentino, L. Jin, M. Melaimi and G. Bertrand, *Chem. Asian J.*, 2015, **10**, 2139-2142.
31. P. De Fremont, N. M. Scott, E. D. Stevens and S. P. Nolan, *Organometallics*, 2005, **24**, 2411-2418.
32. M. J. Lopez-Gomez, D. Martin and G. Bertrand, *Chem. Commun.*, 2013, **49**, 4483-4485.
33. M. Frutos, M. A. Ortuno, A. Lledos, A. Viso, R. Fernandez de la Pradilla, M. C. de la Torre, M. A. Sierra, H. Gornitzka and C. Hemmert, *Org. Lett.*, 2017, **19**, 822-825.
34. K. F. Donnelly, A. Petronilho and M. Albrecht, *Chem. Commun.*, 2013, **49**, 1145-1159.
35. E. C. Keske, O. V. Zenkina, R. Wang and C. M. Crudden, *Organometallics*, 2012, **31**, 6215-6221.
36. C. Mejuto, G. Guisado-Barrios, D. Gusev and E. Peris, *Chem. Commun.* , 2015, **51**, 13914-13917.
37. R. Heath, H. Muller-Bunz and M. Albrecht, *Chem. Commun.*, 2015, **51**, 8699-8701.
38. C. Boehler, D. Stein, N. Donati and H. Gruetzmacher, *New J. Chem.*, 2002, **26**, 1291-1295.
39. D. Canseco-Gonzalez, A. Petronilho, H. Mueller-Bunz, K. Ohmatsu, T. Ooi and M. Albrecht, *J. Am. Chem. Soc.*, 2013, **135**, 13193-13203.
40. J. Bouffard, B. K. Keitz, R. Tonner, G. Guisado-Barrios, G. Frenking, R. H. Grubbs and G. Bertrand, *Organometallics*, 2011, **30**, 2617-2627.
41. L. Hettmanczyk, S. Manck, C. Hoyer, S. Hohloch and B. Sarkar, *Chem. Commun.*, 2015, **51**, 10949-10952.
42. L. Hettmanczyk, S. J. P. Spall, S. Klenk, M. van der Meer, S. Hohloch, J. A. Weinstein and B. Sarkar, *Eur. J. Inorg. Chem.*, 2017, **2017**, 2112-2121.
43. S. Klenk, S. Rupf, L. Suntrup, M. van der Meer and B. Sarkar, *Organometallics*, 2017, **36**, 2026-2035.
44. M. Patra, T. Joshi, V. Pierroz, K. Ingram, M. Kaiser, S. Ferrari, B. Spingler, J. Keiser and G. Gasser, *Chem.Eur. J.*, 2013, **19**, 14768-14772.
45. T. Mosmann, *J Immunol Methods*, 1983, **65**, 55-63.
46. S. S. Mpoke and J. Wolfe, *J. Histochem. Cytochem.*, 1997, **45**, 675-683.
47. D. Ribble, N. B. Goldstein, D. A. Norris and Y. G. Shellman, *BMC Biotechnol.*, 2005, **5**.
48. S. Paglin, T. Hollister, T. Delohery, N. Hackett, M. McMahill, E. Sphicas, D. Domingo and J. Yahalom, *Cancer Res.*, 2001, **61**, 439-444.
49. M. I. Bruce, B. K. Nicholson and O. Bin Shawkataly, *Inorg. Synth.*, 1989, **26**, 324-328.
50. G. A. Price, A. K. Brisdon, K. R. Flower, R. G. Pritchard and P. Quayle, *Tetrahedron Lett.*, 2014, **55**, 151-154.
51. Y. Shi, S. D. Ramgren and S. A. Blum, *Organometallics*, 2009, **28**, 1275-1277.